STATISTICAL NEAR-FAR DETECTION TECHNIQUES FOR GNSS SNAPSHOT RECEIVERS

Sergi Locubiche-Serra, José A. López-Salcedo, Gonzalo Seco-Granados

Universitat Autònoma de Barcelona (UAB), Barcelona, Spain
Email: sergi.locubiche@uab.cat, jose.salcedo@uab.cat, gonzalo.seco@uab.cat

ABSTRACT

In indoor and dense urban environments, Global Navigation Satellite System (GNSS) receivers have to cope with extremely low received power levels. In these circumstances, GNSS receivers become vulnerable to adverse propagation effects such as near-far interference, where acquisition is affected by large cross-correlation peaks because signals from different satellites experience very different attenuation patterns. This translates into a degraded pseudoranges performance, and enters into conflict with the demand for improved positioning accuracy and integrity motivated by the widespread use of GNSS receivers in these scenarios. This paper presents novel low-complexity techniques for near-far detection in high-sensitivity GNSS receivers. These techniques exploit the statistical differences of the acquisition measurements in the presence and in the absence of near-far, and they outperform previously proposed detectors in terms of detection probability. A method to determine the detection threshold for a given probability of false alarm is also presented. Simulations for Galileo E1C signals are used to illustrate the enhanced performance of the proposed algorithms.

Index Terms— Cross-correlation, detection threshold, GNSS, interference detection, near-far.

1. INTRODUCTION

Global Navigation Satellite Systems (GNSS) have experienced an important expansion in the last decade, mainly boosted by the US FCC E911 mandate and the European E112 recommendation on the emergency-call location [1]. Nowadays, GNSS technology is widely used for navigation and precise positioning in safety-critical applications that often require stringent performance, such as maritime, aviation and rail transportations [2].

The availability and positioning accuracy provided by GNSS systems in clear-sky conditions (rural, low-density urban environments) makes them one of the most suitable technologies for the implementation of location based services (LBS) in the massive market of mobile devices. Nonetheless, when operating in indoor or dense urban environments (from now on "indoor" environments), very different from those for which GNSS systems were originally conceived, conventional GNSS receivers face some limitations that still prevent them from being the global LBS enabler. These limitations are mainly due to the high attenuation of signals, non-line-of-sight (NLOS) propagation, multipath and the near-far or cross-correlation problem [3, 4]. This latter case is of paramount importance in indoor scenarios, where high-sensitivity receivers have to deal with very weak signals, and therefore become very vulnerable to interferences.

This work has been partially supported by the Spanish Ministry of Economy and Competitiveness project TEC2014-53656-R.

This paper deals with the near-far detection problem at the acquisition stage in indoor scenarios. In GNSS, satellites transmit a direct-sequence spread-spectrum (DS-SS) signal with a particular pseudorandom code, and one of the first operations performed by GNSS receivers consists in correlating the received signals and the local replicas of the spreading codes. In this sense, the near-far effect is a condition in which a receiver is affected by a strong signal that hampers the detection of a weaker signal [5], since the correlation measurements are distorted by a powerful interference and the wrong signal is acquired. It is particularly relevant in CDMA systems, such as GNSS systems like GPS and the future Galileo. The presence of near-far in GNSS is due to the fact that the cross-correlation between the codes of the strong and weak signals is comparable to the auto-correlation peak of the weak signal that is wanted to be acquired.

The presence of near-far may lead to the following three situations: weak signals from satellites in view are not detected; weak signals from satellites in view are detected but the measured pseudorange has a huge error; a satellite not in view is declared to be present. Thus, near-far detection becomes important in high-sensitivity GNSS receivers; if interfering signals are well detected, the affected satellite can be discarded and the user's position can be estimated correctly by using the rest of available satellites. Although being beyond the scope of this paper, near-far mitigation techniques may be applied in a more sophisticated approach to re-enable the affected satellite. But for this purpose, near-far detection is an initial necessary step before mitigation.

In the literature, many techniques for near-far detection can be found. For instance, multiple-snapshot techniques [6] exploit the frequency and time variability of the near-far interference, which can be detected by observing inconsistent variations along time in the measurements. However, the assumption of the random nature of near-far interference effects is not valid in many situations.

In the literature of single-snapshot techniques, conventional solutions account for different aspects of the correlator output at an observable level. The solution in [7] detects a potential near-far interference by looking at the difference in power of the received signals, but this technique presents the drawback of requiring coarse acquisition of all the received signals. Besides, its performance is poor since near-far interference also depends on the difference in frequency and Time-Of-Arrival (TOA) [8], which translates into a large latency of the position computation. The contribution in [9] proposes a refined version of this detector, which accounts for the power ratio between the largest two correlation peaks. It has low computational complexity, and it presents the advantage of being used after each single signal is acquired, leading to faster localization.

On the other hand, since near-far interference can be modeled as some kind of structured or coloured noise, single-snapshot techniques are low-complexity algorithms that can use the statistical domain of the squared cross-correlation samples for near-far detection, instead of the time and frequency domains. In this regard, it must be

mentioned that, to the authors' knowledge: 1) few efforts have been made in the literature on statistical single-snapshot techniques applied to near-far detection; 2) these are focused on GPS signals. For instance, the publication in [10] proposes a detector based on the different statistical model of the squared cross-correlation measurements for zero and non-zero interference (also known as $\mathcal{H}_0$ and $\mathcal{H}_1$ hypotheses, respectively), and it measures the difference between the probabilities of surpassing a given threshold under each hypothesis. If the difference is high, near-far is present.

The present paper contributes with an exhaustive analysis of statistical single-snapshot techniques for near-far and their characterization in indoor environments for high-sensitivity Galileo receivers, particularly for Galileo E1C signals for civilian use. The detector in [10] is included in the analysis, and a method to determine its optimal threshold is presented. Besides, two exising techniques whose application to near-far detection problems is novel are considered, namely the *Chi-Square Goodness-Of-Fit* and a modified version of the *Kullback-Leibler divergence*. Such techniques fit perfectly into the group of techniques for statistical analyses, and they stand out by their simplicity, thus being very attractive for real handheld GNSS receivers. All these approaches outperform previous detectors [9].

The rest of the paper is organised as follows. In Section 2 the near-far detection problem is presented, and the inherent protection of Galileo E1C spreading codes is evaluated through simulations, since its value needs to be known to assess near-far detection techniques. In Section 3 the techniques studied in this paper are introduced, and a novel method to determine their decision thresholds for a given probability of near-far false alarm is presented. Section 4 shows the simulation results and the enhanced performance of the proposed techniques compared to older methods. Section 5 draws the conclusions.

2. PRELIMINARIES ON NEAR-FAR DETECTION

2.1. Signal model and statement of problem

Let X_p be the 2D time-frequency acquisition matrix containing the squared cross-correlation samples for the pth satellite. Such matrix can also be expressed as $X_p(\tau, f)$. Let $X_p(\tau, f_0)$ be an array from $X_p(\tau, f)$ containing all possible code delays for the Doppler shift f_0 where the signal is located. Let $X_p(\tilde{\tau}, f_0)$ be a reduced version of $X_p(\tau, f_0)$ where the main peak and the samples inside one chip on each side are excluded.

When near-far is absent, the correlator output is dominated by thermal noise for code delays farther than one chip away from the main peak. Therefore, the squared correlation samples follow a χ^2 distribution with $2N_I$ degrees of freedom, where N_I is the number of non-coherent integrations; in this paper $N_I = 3$. On the other hand, when near-far is present, the correlator output is dominated instead by cross-correlation between spreading codes, and in this case the statistics are not perfectly known. These two conditions lead to the signal model in (1).

$$\begin{aligned} X_p(\tilde{\tau}, f_0) &\overset{H_0}{\sim} \chi^2 \\ X_p(\tilde{\tau}, f_0) &\overset{H_1}{\nsim} \chi^2 \end{aligned} \tag{1}$$

Single-snapshot techniques aim at exploiting this uncertainty to detect the presence of near-far by evaluating how much the correlator output affected by near-far differs from a χ^2 distribution. The stronger the near-far effect is, the higher such difference is. For this reason, they are also known as distance to χ^2 distribution techniques.

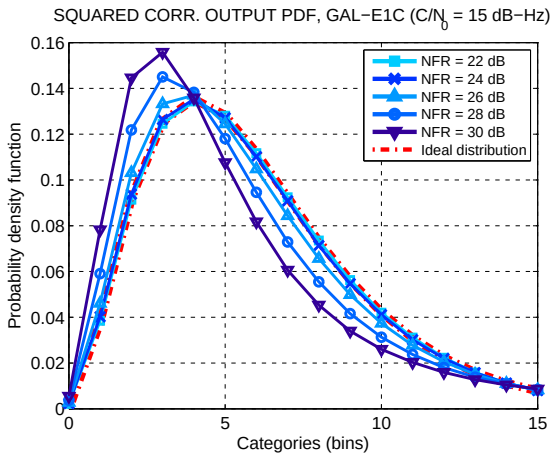

Fig. 1. Mean statistical distributions of squared correlation output samples, for different values of input NFR.

2.2. Inherent protection of spreading codes against near-far

GNSS signals possess an inherent protection against near-far effects, but such protection is limited to a certain upper bound, since the spreading codes used in GNSS are not completely orthogonal. In indoor environments and urban canyons, where signal attenuation can be up to 30 dB when propagating through concrete walls [11], the difference between C/N_0 of desired signals and interfering ones (*i.e.* near-far ratio, NFR) can surpass the protection threshold, and thus the inherent protection is not enough to withstand near-far.

For GPS L1 the protection is about 24 dB for zero Doppler shift in narrow-bandwidth receivers, whereas for any non-zero Doppler shift it decreases to 21.1 dB [12]. For Galileo E1C, the protection can be up to 27 dB for zero Doppler shift. However, no reference to Galileo E1C with non-zero Doppler shift is made in the literature.

In order to evaluate the degradation that the correlator output suffers in the presence of near-far, figure 1 shows an example with the empirical probability density function (pdf) for different values of input NFR. For 50 Monte Carlo iterations and a C/N_0 of 15 dB-Hz, simulations are carried out for random values of Doppler shift following a uniform distribution in the range [-50, 50] Hz. For an input NFR of 22 dB, all empirical distributions match perfectly the ideal near-far-free distribution, whereas for an input NFR of 24 dB a 23.91% of the iterations are affected by near-far, since they differ from the ideal distribution. We can conclude from this that the inherent protection for non-zero Doppler shift Galileo E1C signals is 23-24 dB.

3. STATISTICAL NEAR-FAR DETECTION TECHNIQUES

This section introduces the near-far detectors that are included in the simulation campaign described in Section 4. In general terms, these techniques rely on a given detection threshold to determine whether near-far is present or not. Section 3.4 describes the computation of such detection threshold for a given probability of near-far false alarm.

3.1. Chi-Square Goodness-Of-Fit

The chi-square Goodness-Of-Fit technique is popularly used in economics and biology for hypothesis testing, but it has been rarely used

for near-far detection purposes. It has the objective to test a claim that a set of data follows a particular distribution (in this particular case a χ^2 distribution), and it has the advantage of being applicable to any GNSS modulation.

To apply the chi-square GoF technique to a given satellite p, the pdf of $X_p(\tilde{\tau}, f_0)$ is estimated from correlation measurements and divided into k bins or categories. This gives as a result an observed probability O_i of each ith bin which is compared to the expected probability E_i, which corresponds to the analytical χ^2 distribution in the abscence of near-far. From these, the test statistic for the chi-square GoF is computed as (2) [13].

$$T_{\text{ChiSquareGOF}} = \sum_{i=1}^{k} \frac{(O_i - E_i)^2}{E_i} \tag{2}$$

3.2. Modified Kullback-Leibler divergence

Similarly to the chi-square GoF, the Kullback-Leibler divergence is rarely used in interference detection. It is typically used in digital communications systems, but its application to near-far detection is a novel contribution of this paper. However, a modified version of the KL divergence is presented here, with the objective to enhance the sensitivity of near-far detection.

The modified KL divergence differs from the chi-square GoF only in the way the test statistic is computed. Hence, the same operations in Section 3.1 prior to computing the test statistic of the chi-square GoF apply to the modified KL divergence. After computing the bins of the expected E and observed O distributions, the test statistic for this detector is the KL distance computed as (3),

$$T_{\text{ModifiedKL}} = \sum_{i=1}^{k} \left| O_i \ln\left(\frac{O_i}{E_i}\right) \right| \tag{3}$$

where the absolute value of each element makes the difference to the original KL divergence. It is used so that positive values of the logarithm are not cancelled by negative values in the resulting metric. This ensures that a greater value of distance is obtained.

3.3. Probability of threshold crossing

The threshold crossing technique is based on computing the probability that the correlator output samples exceed a given threshold θ, and it relies on the fact that such probability is higher in the presence of near far. It is computed from the correlator measurements and then compared to the theoretical probability under the $\mathcal{H}_0$ condition. The technique exploits the difference between both probabilities. Therefore, its implementation requires the following steps:

1. Starting with $X_p(\tilde{\tau}, f_0)$, fix a value for the threshold θ.
2. Count the number of samples, N, of $X_p(\tilde{\tau}, f_0)$ that exceed the threshold θ.
3. The test statistic is simply the value of N scaled by the total number of correlation samples N_t (*i.e.* the length of $X_p(\tilde{\tau}, f_0)$), as shown in (4).

$$T_{\text{ProbThCross}} = \frac{N}{N_t} \tag{4}$$

The threshold θ determines whether the difference between both probabilities is high or not, and an optimal value of θ has to be found, so that the technique is fully optimized. The method proposed here consists in choosing the value that maximizes the difference between the mean probabilities of threshold crossings under $\mathcal{H}_0$ and $\mathcal{H}_1$ hypotheses, see (5).

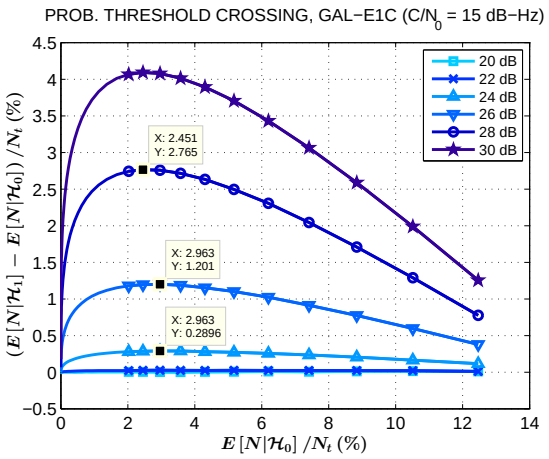

Fig. 2. Difference between mean probabilities of threshold crossing under $\mathcal{H}_1$ and $\mathcal{H}_0$ hypotheses versus mean probability in $\mathcal{H}_0$, for different values of input NFR.

$$\theta_{\text{optimal}} = \arg\max_{\theta} \frac{(E[N|\mathcal{H}_1] - E[N|\mathcal{H}_0])}{N_t} \tag{5}$$

By running simulations with different possible values of θ, the results for different values of input NFR are shown in figure 2. The calculation in (5) presents a maximum value for a given threshold θ, which is very similar for all values of NFR and optimizes the performance of the technique.

3.4. Computation of near-far detection thresholds

Each algorithm presented in this section is characterized by its corresponding test statistic and detection threshold. The decision on the presence of near-far is made by computing such test statistic on the correlation outputs, and further comparing the result to the detection threshold; if the test statistic exceeds the threshold, near-far is declared to be present. Therefore, the value of the detection thresholds needs to be determined. The method proposed here has the particularity that near-far detection thesholds can be set for a given probability of false alarm. The method consists in the following steps:

1. Consider the $\mathcal{H}_0$ condition and compute the test statistic of the detector under test for many Monte Carlo iterations (*i.e.* N_{MC} Monte Carlo iterations), so that many realizations of the test statistic are available. This results in a set of N_{MC} available values of the test statistic.
2. Compute the empirical cumulative density function (cdf) of the previous set of values.
3. Choose a probability of false alarm P_{FA}. The threshold is the value for which the cdf is $(1 - P_{FA})$.

This method ensures that $N/N_{MC} \leq P_{FA}$, where N is the number of realizations whose value exceeds the threshold. These values correspond to false alarm situations, where near-far is detected but the signal is interference-free since the $\mathcal{H}_0$ hypothesis is being considered.

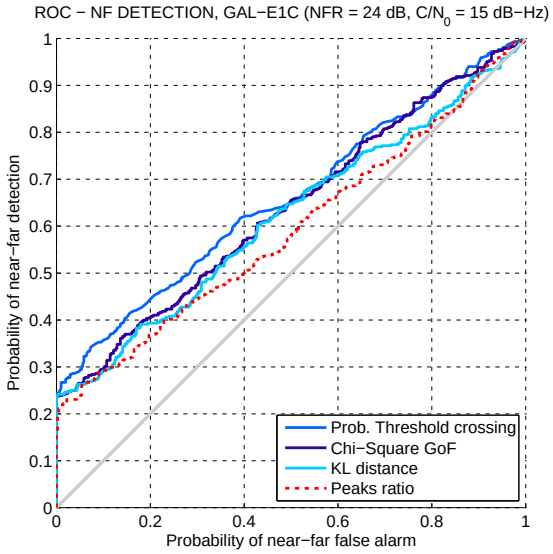

Fig. 3. ROC function of near-far detectors, for input NFR of 24 dB and C/N_0 of 15 dB-Hz.

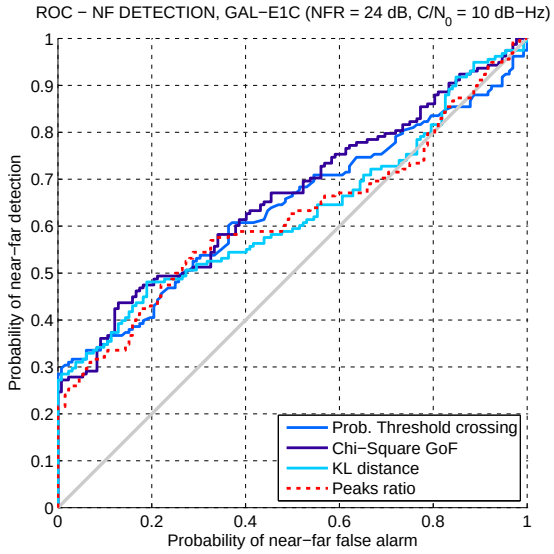

Fig. 4. ROC function of near-far detectors, for input NFR of 24 dB and C/N_0 of 10 dB-Hz.

4. SIMULATION RESULTS

In this section, simulation results are provided to compare the performance of the techniques presented in Section 3. A synthetic signal is used in simulations, which are carried out in the line of high-sensitivity receivers (*i.e.* C/N_0 of 15 dB-Hz and 10 dB-Hz). An input NFR of 24 dB is considered for the following two reasons: 1) it is the limit inherent protection of spreading codes; 2) it is the case where the statistics of the correlation samples are less affected by near-far (*i.e.* detection is more difficult).

Simulation results are provided in terms of ROC functions, where the probability of near-far detection is plotted versus the probability of false alarm. To do so, 500 Monte Carlo iterations are considered, where the Doppler frequency and code phase take uniform random values in the range of [-50, 50] Hz and [0, 4091] chips, respectively, with an estimation resolution of 1 Hz and 0.001 chips. Figure 3 shows, for a C/N_0 of 15 dB-Hz, the ROC functions of the selected near-far detectors, whose performance is compared to the peaks ratio detector in [9]. For the mentioned limit value of input NFR, near-far is detected, starting with probabilities of detection of around 25% for very small probabilities of false alarm.

This is applicable to all techniques, and they all outperform the peaks ratio detector. It shows the worst performance for all probabilities of false alarm (*i.e.* smallest probability of detection). Moreover, its starting probability of detection is around 20%, and since spreading codes fail at 23.91% of the cases at inherently masking near-far, this involves a 3.91% of cases in which near-far is neither masked by spreading codes, nor detected by the technique. On the other hand, the threshold crossing detector shows the best performance (*i.e.* highest probability of detection) for probabilities of false alarm until up to 50%. For this to be valid, the optimal intermediate threshold is chosen, and according to previous figure 2, for an input NFR of 24 dB it is such that $E\left[N|H_0\right]/N_t = 2.963\%$. The performance of the threshold crossing detector is followed by the chi-square GoF and the KL distance detectors.

Simulations are repeated for a C/N_0 of 10 dB-Hz, and the ROC curves of all techniques are shown in figure 4. The results are very similar to those for C/N_0 of 15 dB-Hz. The threshold crossing detector reaches a starting probability of detection around 30%, and it is still the technique which performs best. Nonetheless, in this case the chi-square GoF and the KL divergence detectors show very similar performance to the threshold crossing detector, involving lower computational burden, and thus making them good candidates to substitute traditional interference detectors in software receivers.

5. CONCLUSIONS

This paper has presented an exhaustive analysis of statistical near-far detection techniques for high-sensitivity GNSS receivers. To study them, the inherent protection value of spreading codes with non-zero Doppler shift has been evaluated, and a particular algorithm to determine the detection thresholds for a given probability of near-far false alarm has been used. The chi-square GoF technique and a modified version of the Kullback-Leibler divergence have been presented as novel detectors rarely used in near-far detection. The detector in [10] has been included in the analysis, and a method to determine its optimal threshold has been introduced.

The simulation results have shown that the proposed techniques outperform older approaches [9] in all cases. The probability of threshold crossing detector is the one which performs best, provided that the optimal intermediate threshold is chosen. The detector performs better than the chi-square GoF and the modified KL distance techniques, at the expense of being a more complex technique since the algorithm includes finding such optimal threshold. However, for high-sensitivity receivers (*i.e.* C/N_0 of 10 dB-Hz) the chi-square GoF and the KL detectors perform very similarly to the threshold crossing technique. Thus, both become high-performance low-complexity detectors, with very low power consumption, and these advantages make them very attractive to be implemented in real handheld receivers such as smartphones.

6. REFERENCES

[1] Yilin Zhao, "Mobile phone location determination and its impact on intelligent transportation systems," *Intelligent Transportation Systems, IEEE Transactions on*, vol. 1, no. 1, pp. 55–64, Mar 2000.

[2] M.T. Gamba, B. Motella, and M. Pini, "Statistical test applied to detect distortions of GNSS signals," in *Localization and GNSS (ICL-GNSS), 2013 International Conference on*, June 2013, pp. 1–6.

[3] F. van Diggelen, "Indoor GPS theory and implementation," in *Position Location and Navigation Symposium, 2002 IEEE*, 2002, pp. 240–247.

[4] G. Lachapelle, H. Kuusniemi, D.T.H. Dao, G. MacGougan, and M.E. Cannon, "HSGPS Signal Analysis and Performance Under Various Indoor Conditions," *NAVIGATION, Journal of The Institute of Navigation*, vol. 51, no. 1, pp. 29–44, Spring 2004.

[5] Theodore Rappaport, *Wireless Communications: Principles and Practice*, Prentice Hall PTR, Upper Saddle River, NJ, USA, 2nd edition, 2001.

[6] P.G. Mattos, "Solutions to the Cross-Correlation and Oscillator Stability Problems for Indoor C/A Code GPS," *Proceedings of the 16th International Technical Meeting of the Satellite Division of The Institute of Navigation (ION GPS/GNSS 2003)*, pp. 654–659, September 2003.

[7] P.H. Madhani, P. Axelrad, K. Krumvieda, and J. Thomas, "Application of successive interference cancellation to the GPS pseudolite near-far problem," *Aerospace and Electronic Systems, IEEE Transactions on*, vol. 39, no. 2, pp. 481–488, April 2003.

[8] B.W. Parkinson and J.J. Spilker, *Global Positioning System: Theory and Applications*, vol. 1 of *Progress in astronautics and aeronautics*, American Institute of Aeronautics & Astronautics, 1996.

[9] G. Lopez-Risueno and G. Seco-Granados, "Detection and Mitigation of Cross-Correlation Interference in High-Sensitivity GNSS Receivers," in *Personal, Indoor and Mobile Radio Communications, 2007. PIMRC 2007. IEEE 18th International Symposium on*, Sept 2007, pp. 1–5.

[10] G. Lopez-Risueno and G. Seco-Granados, "CN0 estimation and near-far mitigation for GNSS indoor receivers," in *Vehicular Technology Conference, 2005. VTC 2005-Spring. 2005 IEEE 61st*, May 2005, vol. 4, pp. 2624–2628 Vol. 4.

[11] F.D. Nunes, F.M.G. Sousa, and N. Blanco-Delgado, "A VDLL Approach to GNSS Cell Positioning for Indoor Scenarios," *Proceedings of the 22nd International Technical Meeting of The Satellite Division of the Institute of Navigation (ION GNSS 2009)*, pp. 1690–1699, September 2009.

[12] E. Kaplan and C. Hegarty, *Understanding GPS: Principles and Applications, Second Edition*, Artech House mobile communications series. Artech House, 2005.

[13] M. Pini, B. Motella, and M.T. Gamba, "Detection of Correlation Distortions Through Application of Statistical Methods," *Proceedings of the 26th International Technical Meeting of The Satellite Division of the Institute of Navigation (ION GNSS+ 2013)*, pp. 3279–3289, September 2013.